Transactions of the SMiRT 27
Yokohama, Japan, March 3-8, 2024
Division IV

SEISMIC RESPONSES OF BASE-ISOLATED NUCLEAR POWER PLANTS WITH CONSIDERATIONS OF IMPACT

Ching-Ching Yu[1], Andrew S. Whittaker[2], Benjamin D. Kosbab[3], and Payman Khalili Tehrani[4]

[1] Former Postdoctoral Associate, University at Buffalo, Buffalo, NY (cyu23@buffalo.edu)
[2] SUNY Distinguished Professor, University at Buffalo, Buffalo, NY
[3] Principal, Simpson Gumpertz & Heger, Atlanta, GA
[4] Director of Engineering, SC Solutions, CA

ABSTRACT

Earthquake shaking more intense than that used to size the horizontal clearance between a base-isolated reactor building and a near-rigid perimeter moat wall will result in *hard impact*, producing high-frequency, high-amplitude accelerations in the building and on its internal equipment. The paper explores the merits of avoiding hard impact, by engineering a compliant restraint between a base-isolated building and a surrounding moat wall. Dynamic analysis is performed for an archetype reactor building supported by a linear elastomeric isolation system. Extreme horizontal shaking with a peak ground acceleration of 1 g is used as the input motion: sufficient to result in impact. A commercial-off-the-shelf marine fender with well-defined stiffness and damping is used here as the compliant restraint, installed in the horizontal load path between the base-isolated building and the moat wall, resulting in soft impact. The isolation-system displacements, accelerations on the building and equipment, and shear forces in the walls of the building are presented to illustrate the effectiveness of engineering soft impact.

INTRODUCTION

Figure 1 presents a reactor building supported by a seismic isolation system. The isolators (black solid squares) are shown installed on reinforced concrete pedestals, below the basemat and above the foundation. The 2D (horizontal) isolation system increases the fundamental period of the reactor building, which substantially reduces in-structure accelerations generated by ground shaking but increases displacements above the foundation. Nearly all the lateral displacement is in the isolation system, with negligible drift above the basemat.

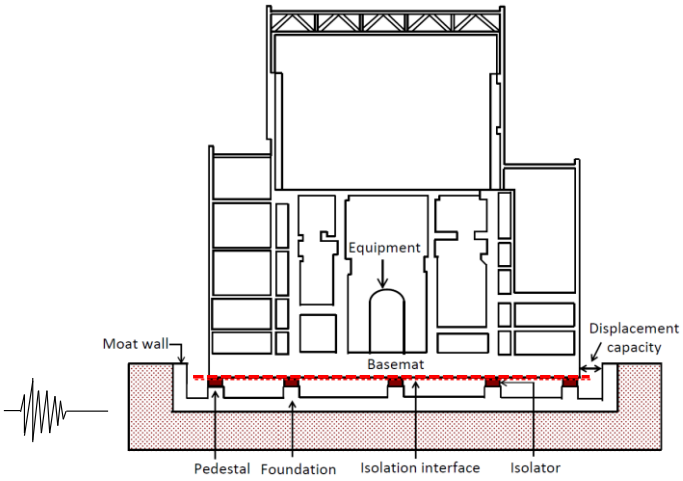

Figure 1. Base isolated building (Kammerer *et al.* 2019)

The horizontal displacement of the isolated reactor building may be limited by the proximity of adjacent construction, such as the reinforced concrete moat wall shown in Figure 1. The basemat will impact the moat wall if the earthquake-induced horizontal displacement is greater than the

clearance (noted as Displacement capacity in Figure 1). The minimum horizontal clearance to avoid impact of the base-isolated building on the moat wall can be established (Yu *et al.* 2022; 2023a) for a user-specified annual frequency of exceedance, site and isolation system. However, the responses of the building and its equipment for earthquake shaking more intense than that used to size the horizontal clearance may need to be considered in support of risk calculations.

A base-isolated building impacting a near-rigid moat wall may result in high-frequency, high-amplitude shaking in the building, if the impact velocity is significant (Masroor and Mosqueda 2013; Sarebanha *et al.* 2018): *hard* impact. To eliminate the negative effect of hard impact, a compliant restraint can be installed in the horizontal load path between the base-isolated building and the moat wall, resulting in *soft impact*. The benefits of engineering a soft impact for an isolated reactor building to avoid hard impact were studied in Yu *et al.* (2023c) using analytical and numerical tools for a single degree-of-freedom model. A commercial off-the-shelf marine fender, with well-defined stiffness and damping, was used as the compliant restraint attached to a near-rigid moat wall surrounding the base-isolated building. The use of the compliant restraint resulted in much smaller accelerations on the basemat (i.e., the degree of freedom).

This paper explores the merits of soft impact using a 3D finite element model of an isolated reactor building. A linear elastomeric isolation system is considered but that is not a limitation of the study because the focus is the restraint. Two types of restraint are used to restrict the displacement of the isolated building: 1) near-rigid moat wall (hard restraint), and 2) marine fender (compliant restraint). Two-component horizontal motions with a peak ground acceleration of 1 g, sufficient to result in impact, are used as the inputs. Isolation-system displacements, in-structure accelerations on the building and equipment, and shear forces in the walls of the building are reported to enable the reader to judge the effectiveness of *soft* impact. (Another strategy to avoid hard impact is adding damping to the isolation system to reduce the horizontal displacement and the likelihood of contacting the moat wall, which is explored in Yu *et al.* (2023b).)

BASE-ISOLATED NUCLEAR POWER PLANT

Figure 2 presents the finite element model of the nuclear reactor building and equipment built in SAP2000 (CSI 2020). The model was used and described in detail in Yu *et al.* (2023a), and a brief summary is provided below. Figure 2a presents the key dimensions of the building. The out-to-out plan dimensions are 25 m $\times$ 25 m, and the height from the bottom of the basemat to the ridge is 33 m. The reactor building includes four floors: a reinforced concrete (RC) basemat (grey), a suspended RC floor (green), and two composite floors (yellow). The suspended RC floor is supported around its perimeter by 1.2 m-thick RC walls (orange), sized for wind-borne missile impact. The building is framed in structural steel above the upper composite floor. The reactor shield is a cylindrical, reinforced concrete wall (shaded pink) supported on the basemat shown in Figure 2b. The basemat, suspended RC floor, composite floors, walls, and reactor shield are modeled using linear elastic shell elements. The structural steel framing is modeled using linear elastic line elements. Generic mechanical properties for uncracked concrete (steel) are assigned to the shell (line) elements. The part of the building below the top of the suspended RC floor and reactor shield head is assumed to be safety-related and houses safety-related equipment. The building above the suspended RC floor, namely, the steel framing, the composite floors, and the crane, is assumed to be non-safety related. Safety-related equipment is shown in Figure 2b: a reactor vessel (RV), a reactor vessel auxiliary cooling system (RVACS), and 4 primary heat exchangers (PHXs). They are assumed to be manufactured using stainless steel and filled with molten salt. Oscillators with horizontal frequencies of 10 and 20 Hz and negligible mass are attached to the reactor head to represent head-mounted equipment. A 40-tonne gantry crane is installed on the steel frame: the mass of 27 tonnes is evenly distributed to the steel columns on the *y-z* faces at the elevation of 28 m noted in Figure 2a.

The weight of the reactor building, including the reactor shield, gantry crane, equipment, and superimposed dead and live loads on the slabs, is 8,920 tonnes. Eigenmodes are calculated for the reactor building assumed to be conventionally founded. Four percent of critical damping is assigned

to all modes. The modes with the greatest effective mass are at 10 Hz in the *x* and *y* directions and 24 Hz in the *z* direction. The 10-Hz modes are associated with the horizontal displacements of the RC walls, suspended RC floor, and reactor shield, and the 24-Hz mode is associated with the vertical displacements of the suspended RC floor, axial extension of the reactor shield wall, and breathing of the RC walls. The first horizontal and vertical modal frequencies of the RV are 12 Hz and 37 Hz, respectively.

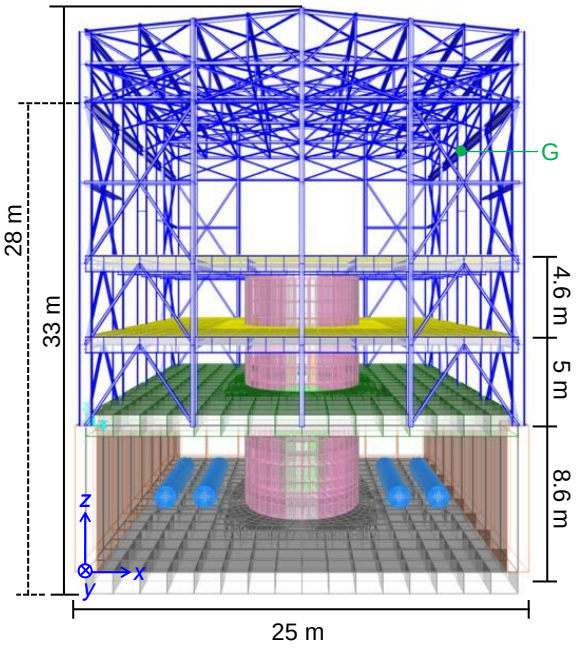

(a) building (RC wall on the +*y* face removed from view)

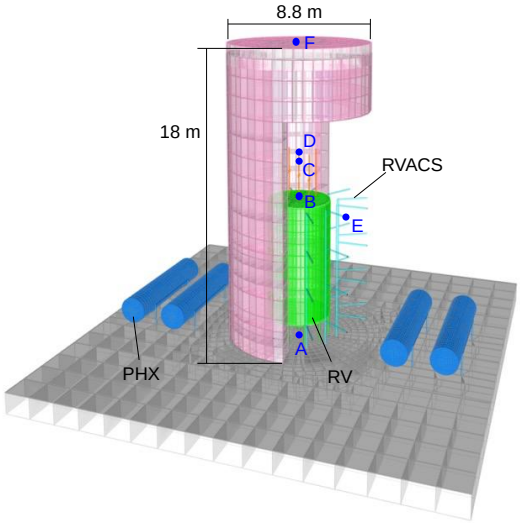

(b) basemat, reactor shield, and safety-related equipment

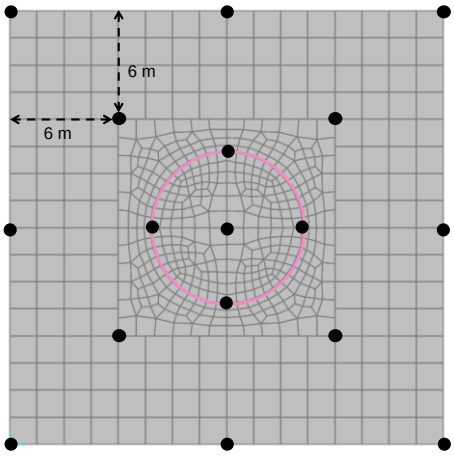

(c) 17 isolators, noted as black solid circles

Figure 2. Reactor building, equipment, and isolation system

The building is supported by a 2-sec linear isolation system including 17 identical natural rubber (elastomeric) isolators, as shown in the layout of Figure 2c. The layout is not optimized. Given the horizontal period of 2 seconds and the superstructure mass of 8,920 tonnes, the horizontal stiffness of the isolation system, k_{iso}, is 8.8×10^4 kN/m. Assuming 5% of critical damping in the elastomer, the damping coefficient, c_{iso}, is 2.8×10^3 kN-s/m. The 17 isolators (i=1 to 17) are simulated explicitly using linear link elements (SAP2000) in the building model with identical properties: $k_{iso,i} = k_{iso}/17$ and $c_{iso,i} = c_{iso}/17$ in the two horizontal directions.

CLEARANCE AND DISPLACEMENT RESTRAINT

Two displacement restraints on the isolation system are considered: 1) a near-rigid moat wall, termed a hard restraint, and 2) a heavy-duty, commercial-off-the-shelf, marine fenders attached to the moat wall, termed a compliant or soft restraint. The clearance, e, between the basemat and either of the two restraints is set to 200 mm. Figure 3 presents a (not-to-scale) plan view of the basemat as a shaded grey square, the moat wall as solid black lines (panels a and b), and the fenders as yellow (panel b). The horizontal principal axes of the building are denoted x and y. To attach the fenders to the moat wall and provide a clearance of 200 mm, the distance between the face of the building and the moat wall is increased by the width of the fender, as noted in Figure 3b.

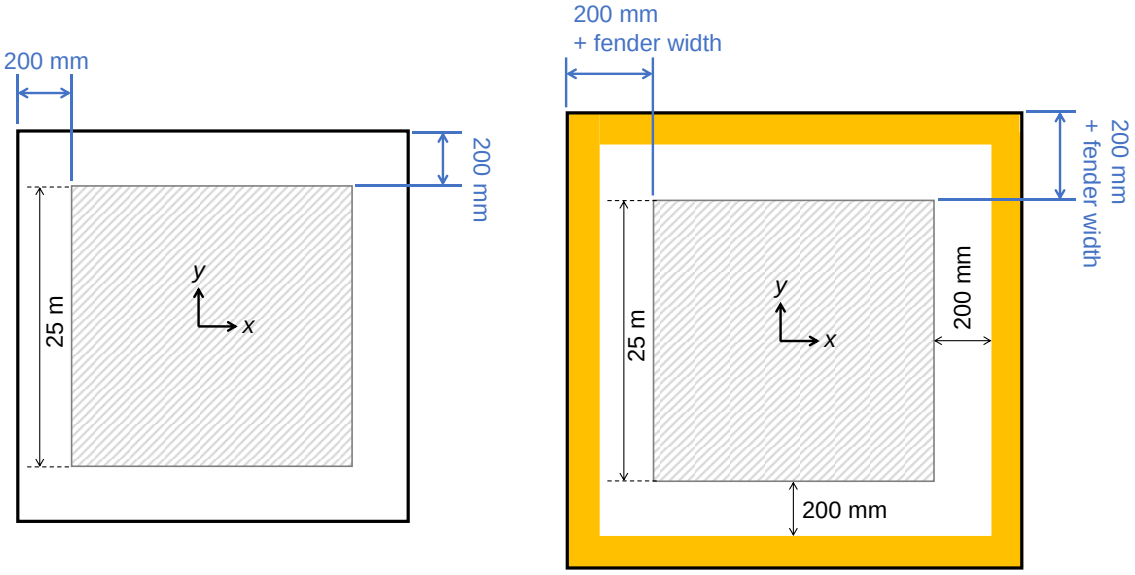

(a) hard restraint (b) compliant restraint

Figure 3. Plan view of the isolated building (hatched), near-rigid moat walls (solid line), and compliant displacement restraint (yellow), not to scale

The lateral elastic stiffness for the hard restraint in compression is assumed to be $k_e = 2000$ kN/mm ($\geq 20\,k_{iso}$), which is reasonable for a 25-m long, 1-m thick, cantilever reinforced concrete moat wall backed by soil. (A bounding analysis for the lateral stiffness of a moat wall-soil assembly is not considered.) Figure 4 presents the horizontal force-displacement (lateral deformation, Δ) relationship for the hard restraint in blue, for a displacement less than 30 mm. (The vertical axis in Figure 4 is discontinued between 20 and 50 MN.) Five percent of critical damping is assumed for the hard restraint: c_e = 13.4 kN-s/mm, characterized using the superstructure mass of $m = 8{,}920$ tonnes. If the moat wall is near-rigid, the lateral stiffness of the fender-wall assembly is that of the fender only. The force-displacement relationship of the fender is presented in Figure 4 using a yellow line. The compressive stiffness is trilinear: $k_{e1} = 100$ kN/mm for $0 \leq \Delta < 25$ mm, $k_{e2} = 300$ kN/mm for 25 mm $\leq \Delta < 45$ mm, and $k_{e3} = 700$ kN/mm for $\Delta > 45$ mm. The three stiffnesses are based on test data (ShibataFenderTeam Inc. 2022) and finite element analysis (Yu *et al.* 2023c). Five percent of critical damping is assumed for the fender: $c_e = 3$ kN-s/mm, determined by $k_{e1} = 100$ kN/mm and $m = 8920$ tonnes. (With constant $c_e = 3$ kN-s/mm, if $\Delta > 25$ mm, both tangent and secant stiffnesses are greater than k_{e1}, and the damping ratio is less than 5%.) The mechanical properties of the fender (i.e., the compliant restraint) are not optimized for either the building or the assumed ground shaking. Table 1 summarizes the clearance and properties of the hard and compliant restraints.

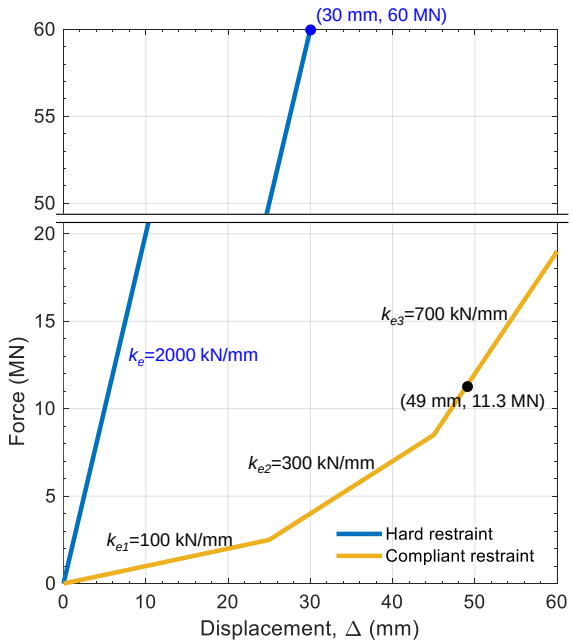

Figure 4. Force-displacement relationship, linear stiffness for hard restraint, tri-linear stiffness for the compliant restraint, in compression

Table 1: Clearance and properties of the hard and compliant restraints in compression

Hard restraint	e	200 mm
	k_e	2000 kN/mm
	c_e	13.4 kN-s/mm
Compliant restraint	e	200 mm
	k_e	k_{e1} = 100 kN/mm for 0 to 25 mm k_{e2} = 300 kN/mm for 25 to 45 mm k_{e3} = 700 kN/mm for 45 + mm
	c_e	3 kN-s/mm

NUMERICAL MODEL FOR IMPACT ANALYSIS

Figure 5a describes the modeling approach used for the impact analysis of the base-isolated nuclear power plant (NPP). This approach, which models the reactor building (denoted as NPP in Figure 5a), internal equipment, and isolation system (green in Figure 5a) explicitly, is extended from the single-degree-of-freedom model proposed in Yu *et al.* (2023c). The approach was verified in Yu *et al.* (2023b) using analytical solutions presented in (Yu *et al.* 2023c). Localized impact on the perimeter moat wall is not addressed. The displacement restraint is modeled using the orange impact elements shown in Figure 5a, per building face, at the level of the basemat (hatched). Each impact element includes a spring, k_e, and a dashpot, c_e. A gap element, shown in blue in Figure 5a, is introduced between the basemat and each impact element. These gap elements are assigned zero stiffness in tension for all deformation, Δ, and in compression for $\Delta < e$. For $\Delta \geq e$ in compression, the gap elements are *numerically rigid* by assigning a significant stiffness.

Figure 5b presents the model of the reactor building for the impact analysis. Link elements are used to model the soft and hard restraints and the clearance. The link elements for the restraints, namely, impact elements, are shown in orange in Figure 5b, at 6.25 m on center, and opposite the basemat. The five impact elements per building face are assigned an axial stiffness and damping coefficient to recover the force-displacement relationships defined in Figure 4 and Table 1. The hard restraint is modeled using *linear* links (per SAP2000) with $k_{e,i} = k_e/5$ and $c_{e,i} = c_e/5$. The compliant

restraint is modeled using the *Multi-linear Elastic* links (per SAP2000) for the trilinear stiffness, $k_{e1,i} = k_{e1}/5$, $k_{e2,i} = k_{e2}/5$, and $k_{e3,i} = k_{e3}/5$, and the *damper-exponential* links (per SAP2000) for the damping coefficient, $c_{e,i} = c_e/5$. One end of the impact elements is fixed at the ground and the other end is attached to the gap elements shown as blue in Figure 5b. The gap elements are used to model the clearance of 200 mm between the basemat and restraint. Zero stiffness is assigned to the gap elements for all Δ in tension and $\Delta < 200$ mm in compression. For $\Delta \geq 200$ mm in compression, the stiffness is $2+$ orders of magnitude greater than the linear stiffness, $k_{e,i}$, for the hard impact elements and the third-slope stiffness, $k_{e3,i}$, for the soft impact elements.

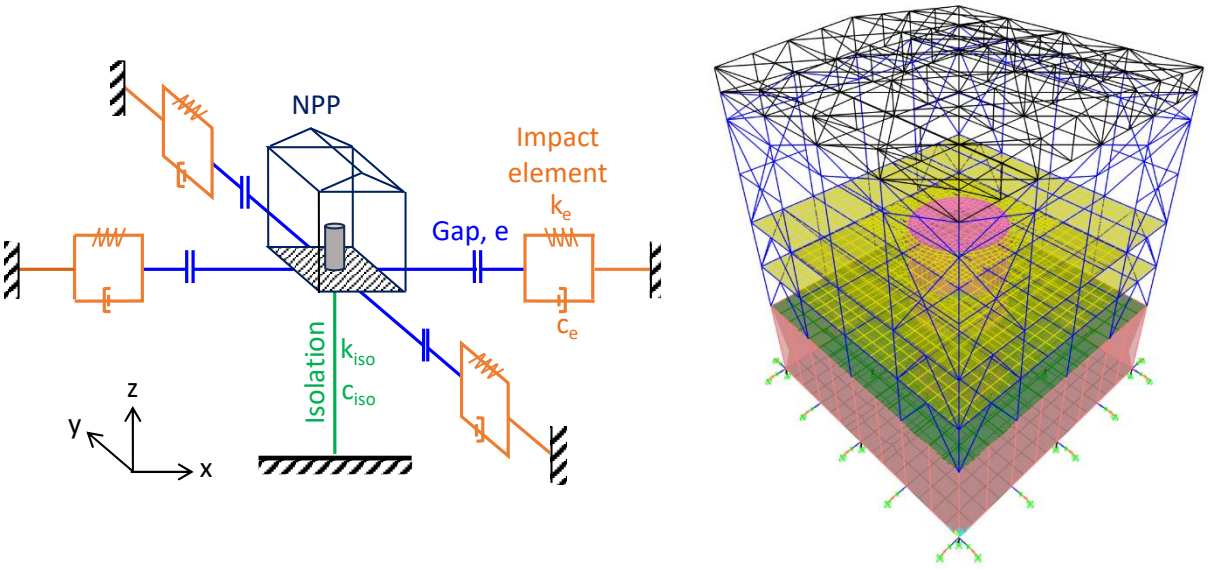

(a) modeling approach and parameters

(b) isolated building with impact and gap elements

Figure 5. Numerical model of the base-isolated reactor building with considerations of impact

DYNAMIC ANALYSIS AND RESULTS

Introduction

Response-history analysis of the base-isolated reactor building is performed for two-component horizontal input motions with a peak ground acceleration (PGA) of 1 g. Table 2 lists the three analysis cases. Case 0 is the analysis of the isolated building with no displacement restraint and it is used hereafter as a benchmark. The mean maximum isolation-system displacement for case 0 and 1-g ground shaking is greater than 200 mm (as presented in Table 3). In cases 1 and 2, the hard and compliant restraints with a clearance of 200 mm from each building face are included in the model, which results in hard and soft impact, respectively.

Table 2: Analysis cases

Case	Displacement restraint	Clearance (mm)
0	None (unrestricted)	No limit
1	Hard	200
2	Compliant	

Ground motion time series

Thirty sets of two-component horizontal input motions are generated for the response-history analysis. The thirty pairs of ground motions are spectrally matched to a uniform hazard response spectrum (UHRS) using RSPMatch2005 (Hancock *et al.* 2006). The UHRS is the geomean of two horizontal components, and is developed using hazard data published by the United States Geological Survey

(USGS) (2018) for an assumed site, return period, and site class. Figure 6 presents the UHRS (yellow) and the spectra for the 30 inputs (grey) in the two horizontal directions, for 5% of critical damping. The peak ground acceleration (PGA) is 1 g. This UHRS is representative of extreme ground motion that reasonably approximates two cases: 1) 25,000-year return-period shaking on a soft-rock or stiff-soil site in the Central and Eastern US (CEUS), and 2) 10,000-year shaking on a soft rock site in the Western US (WUS).

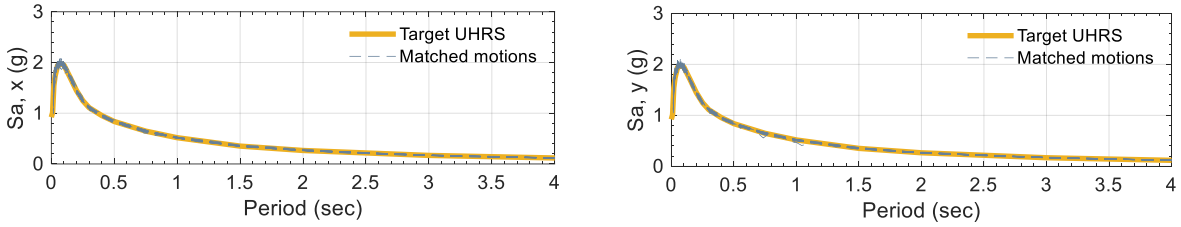

(a) *x* direction (b) *y* direction

Figure 6. Acceleration response spectra (*Sa*) for input motions, 5% of critical damping, PGA = 1 g

Analysis results and observations

Isolation-system displacements, in-structure accelerations on the building and equipment, and shear forces in the walls of the building are reported for the 3 cases of Table 2. Table 3 presents the means of maximum horizontal isolation-system displacements for the 30 inputs. The mean maximum displacements along the two principal axes (*x* and *y*) for each case are essentially identical for each case. The square root of the sum of the squares (SRSS) of the two horizontal components, namely, peak displacements, is calculated at every time step for each input, and the mean of the 30 maxima is presented in the last column.

Table 3: Mean maximum horizontal isolation-system displacements, units of mm, 30 inputs, PGA = 1g

Case	Description	*x*	*y*	SRSS (peak)
0	Unrestricted, no impact	256	257	304
1	Hard impact	230	230	278
2	Soft impact	249	248	296

The mean maximum unrestricted horizontal displacement along the two principal axes of the building (case 0) is 257 mm: sufficient to result in impact if the clearance was set to 200 mm (cases 1 and 2). The maximum isolation-system displacements for case 1 (2) are reduced by approximately 26 mm (7 mm), associated with 30 (49) mm of deformation in the hard (compliant) restraint. These deformations generate compresion forces of 60 MN and 11.3 MN on the hard and compliant restraints, respectively, as identified in Figure 4.

The most seismically vulnerable components in a reactor building are equipment, which generally have frequencies of 5 Hz and higher. To judge the efficacy of the different strategies to mitigate the effects of hard impact, accelerations are monitored and reported at 7 locations on the building and equipment, identified using green and blue solid circles in Figure 2:

- A: center of the basemat, at the point of support of the reactor vessel
- B: center of the reactor head, at the point of support of head-mounted equipment
- C: 10 Hz oscillator mounted on the reactor head
- D: 20 Hz oscillator mounted on the reactor head
- E: upper support of RVACS, inside of shield wall
- F: center of the head to the reactor shield structure
- G: point of attachment of the bridge crane on the steel frame

Table 4 presents mean maximum peak horizontal accelerations at the 7 locations for the 30 inputs for each analysis case. The peak horizontal accelerations are calculated as the SRSS of the two horizontal components at every time step for each input. Figure 7 presents the mean of 30 geomean horizontal response spectra (*Sa*) at the center of the basemat (location A) and the center of the reactor head (location B) for each analysis case. The spectra are calculated using 5% of critical damping at frequencies between 0.1 and 100 Hz.

Table 4: Mean maximum peak horizontal acceleration, SRSS of the two components, units of g, 30 inputs, PGA = 1g, seven locations

		Monitoring locations						
Case	Description	A	B	C	D	E	F	G
0	Unrestricted, no impact	0.31	0.32	0.34	0.32	0.31	0.32	0.33
1	Hard impact	1.16	1.34	2.50	2.16	1.10	1.51	2.35
2	Soft impact	0.44	0.46	0.58	0.52	0.44	0.47	0.55

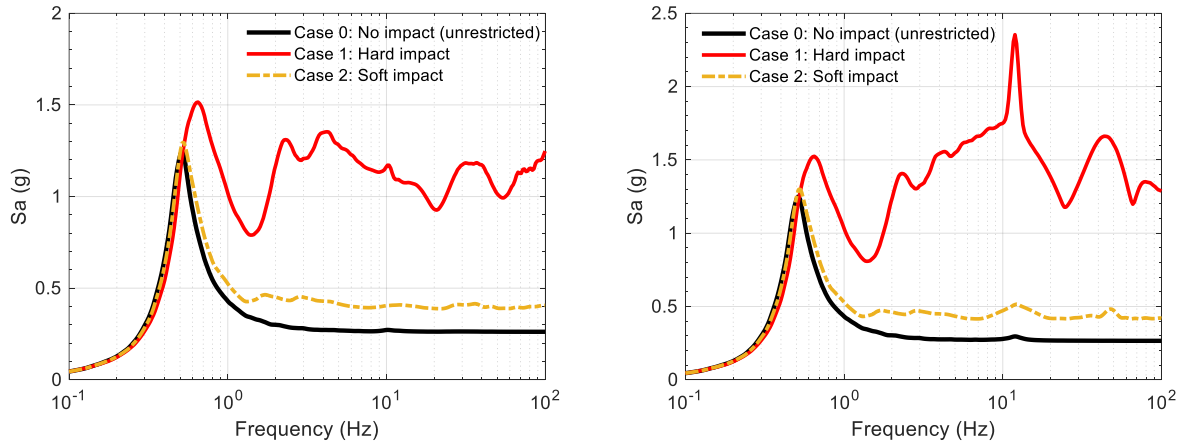

(a) location A, basemat (b) location B, reactor head

Figure 7. Mean response spectra, geomean horizontal, two locations, 5% of critical damping, 30 inputs, PGA = 1 g

The spectra at locations A and B shown in Figure 7 for the unrestricted isolation system (case 0; black lines) are essentially identical. The two spectra peak at the isolation-system frequency of 0.5 Hz, which is of no consequence to equipment; the spectral ordinates are essentially constant for frequencies greater than 2 Hz. Per Table 4, the maximum accelerations at the 7 monitoring locations for case 0 are all equal to approximately one-third of the PGA.

The accelerations for cases 0, 1, and 2 presented in Table 4 and Figure 7 can be compared to identify the deleterious effects of hard impact and the benefits of engineering soft impact. Per Table 4, hard impact (case 1) increases the maximum accelerations at the 7 locations significantly: 4 to 8 times the case-0 counterparts. Replacing the hard restraint (case 1) with the soft restraint (case 2) reduces the maximum accelerations by 60% to 80% at the 7 locations. Per Figure 7, the hard impact (case 1; red lines) results in high-frequency, high-amplitude accelerations. For frequencies greater than 5 Hz, the spectral amplitude for case 1 and location A (B) is 3 to 5 (5 to 9) times the case-0 counterpart. The soft impact (case 2; yellow lines) does not significantly amplify the high-frequency spectral demands at these locations: approximately 1.5 times those for case 0 for frequencies greater than 5 Hz. The hard (soft) impact shifts the first spectral peak from 0.5 Hz to 0.64 (0.53) Hz. The shifted frequency is a function of the stiffnesses of the isolation system and restraint, isolation-system displacement, and clearance between the building and restraints. Yu *et al.* (2023c) presents analytical solutions for the shifted frequency and they were used to verify the modeling approach for impact analysis in Yu *et al.* (2023b). On the basis of data presented in Table 4 and Figure 7, the benefits of avoiding hard impact (case 1) by engineering a soft impact is evident.

The perimeter walls shown in orange in Figure 2a are used to provide a load path for gravity, seismic, and wind forces, a barrier against the ingress of wind-borne missiles, and confinement in the event of release of radionuclides. Net shearing forces, V , in the x and y directions, in the walls normal to the y and x directions, respectively, immediately above the basemat, are reported. Table 5 presents mean maximum shearing forces in kN (rounded to the nearest 100), % of the reactive building weight W = 8920 tonnes, and average in-plane shear stress τ in MPa. The in-plane shear stress τ is computed by dividing a half of the reported mean maximum shearing force ($0.5V$; two walls in each direction) by the wall length (25 m) and thickness (1.2 m). Note that the limiting design shear stress per ACI 318-19 (2019) is 2.62 MPa (= 380 psi) for 4000 psi concrete. The ratios of demand-to-capacity (D/C) are computed as the reported shear stresses τ divided by 2.62 MPa and presented in Table 5.

Table 5. Mean maximum shearing forces, % of the reactive building weight, and in-plane shear stress in perimeter walls, ratios of demand-to-capacity (= 2.62 MPa), 30 inputs, PGA = 1g

		x				*y*			
Case	Description	V (kN)	%W	τ (MPa)	D/C	V (kN)	%W	τ (MPa)	D/C
0	Unrestricted, no impact	12,400	14	0.21	0.08	12,400	14	0.21	0.08
1	Hard impact	44,000	50	0.73	0.28	43,000	49	0.72	0.27
2	Soft impact	18,000	21	0.30	0.11	17,800	20	0.30	0.11

All in-plane shear stresses are significantly less than the limiting design value (capacity) of 2.62 MPa. The demand-to-capacity ratios in the perimeter shear walls for all 3 cases are low (D/C<0.3), in part because the wall thickness was sized to protect against wind-borne missile impact. Accordingly, no seismic penalty is incurred for the construction of the shear walls in the reactor building supported by the isolation systems and displacement restraints considered here for a clearance of 200 mm. The residual crack widths at these ratios of demand-to-capacity will be narrow (Rivera and Whittaker 2019). Comparing case 2 to case 1, using the compliant restraint for eliminating hard impact reduces the shear stresses by more than 50%.

SUMMARY AND CONCLUSIONS

The horizontal displacement of an isolated reactor building may be limited by the presence of adjacent construction (e.g., moat wall) in the event of shaking more intense than design basis. If the unrestricted horizontal displacement of the isolation system is greater than the clearance, the reactor building will impact the adjacent construction: *hard impact*. Hard impact may result in high-frequency, high-amplitude accelerations if the impact velocity is high. This paper confirms the negative effect of hard impact identified in prior studies (Masroor and Mosqueda 2013; Sarebanha *et al.* 2018), and propose engineering *soft impact* for eliminating hard impact by introducing a compliant displacement restraint between the building and adjacent construction.

Dynamic analysis of a base-isolated reactor building is performed to explore the merit of using a compliant restraint. The reactor building is supported by a 2-sec linear elastomeric isolation system. A clearance of 200 mm is set between the building and the two types of displacement restraint: 1) near-rigid moat walls (hard restraint), and 2) marine fenders (compliant restraint). The finite element model for the dynamic analysis includes the reactor building, internal equipment, isolation system, and displacement restraints explicitly. Thirty pairs of horizontal input motions with a PGA of 1 g, representing extreme earthquake shaking, are used for the dynamic analysis.

Three analysis cases are considered for the 1-g inputs: 0) no restraint, namely, isolation-system displacement is unrestricted, 1) hard restraint, and 2) compliant restraint. Mean maximum isolation-system displacements, in-structure accelerations at 7 locations, and shear forces in the walls of the building are reported. Limiting the horizontal displacement of the isolation system by impact on the hard restraint serves the intended purpose but at the expense of high in-structure accelerations.

The introduction of the compliant restraint limits the horizontal displacement of the isolation system with no meaningful difference in in-structure accelerations from case 0: the unrestricted horizontal movement of the isolation system. Based on the presented data, the benefits of avoiding hard impact by engineering a soft impact is evident. (Another strategy to avoid hard impact is adding damping to the isolation system to reduce the horizontal displacement and the likelihood of contacting the moat wall, which is explored in Yu *et al.* (2023b).)

ACKNOWLEDGMENTS

The information, data, and work presented herein were funded in part by the U.S. Department of Energy, under Award Number DE-NE0008932. The authors thank Benjamin M. Carmichael, Brandon M. Chisholm, and Jason P. Redd of Southern Company, Brian I. Song of Kairos Power, Chandrakanth Bolisetti of the Idaho National Laboratory, and Dan Murphy of the ShibataFenderTeam for their contributions to this study. The views and opinions of the authors expressed herein do not necessarily state or reflect those of the United States Government, the Idaho National Laboratory, Southern Company, Kairos Power, or the ShibataFenderTeam.

REFERENCES

American Concrete Institute (ACI) (2019). "Building code requirements for structural concrete and commentary." *ACI 318-19*, ACI, Farmington Hills, IL.

Computers and Structures (CSI) (2020). "SAP2000 Version 22.1.0." CSI, Walnut Creek, CA.

Hancock, J., Watson-Lamprey, J., Abrahamson, N. A., Bommer, J. J., Markatis, A., McCoyh, E., and Mendis, R. (2006). "An improved method of matching response spectra of recorded earthquake ground motion using wavelets." *Journal of Earthquake Engineering*, 10(spec01), 67-89.

Kammerer, A. M., Whittaker, A. S., and Constantinou, M. C. (2019). "Technical considerations for seismic isolation of nuclear facilities." *NUREG/CR-7253*, Nuclear Regulatory Commission (NRC), Washington D.C.

Masroor, A., and Mosqueda, G. (2013). "Impact model for simulation of base isolated buildings impacting flexible moat walls." *Earthquake Engineering and Structural Dynamics*, 42(3), 357-376.

Rivera, J., and Whittaker, A. S. (2019). "Damage and peak shear strength in low-aspect-ratio reinforced concrete shear walls." *Journal of Structural Engineering*, 145(11), 04019141.

Sarebanha, A., Mosqueda, G., Kim, M. K., and Kim, J. H. (2018). "Seismic response of base isolated nuclear power plants considering impact to moat walls." *Nuclear Engineering and Design*, 328, 58-72.

ShibataFenderTeam Inc. (2022). "Extruded fenders.", <https://www.shibata-fender.team/en/products/extruded-fenders.html>. (May, 2022).

United States Geological Survey (USGS) (2018). "Hazard curves for the 2018 update of the U.S. National Seismic Hazard Model." <https://www.sciencebase.gov/catalog/item/5d559795e4b01d82ce8e3fef>. (Feb, 2021).

Yu, C.-C., Carmichael, B. M., Redd, J. P., Chisholm, B. M., Peres, M. W., Song, B. I., Denman, M., Bolisetti, C., and Whittaker, A. S. "Achieving a seismic risk target for a seismically isolated advanced reactor." *Proc., 2022 American Nuclear Society (ANS) Winter Meeting*.

Yu, C.-C., Mir, F. U. H., Carmichael, B. M., Chisholm, B. M., Redd, J., Bolisetti, C., and Whittaker, A. S. (2023a). "Guidelines for implementing seismic base isolation in advanced nuclear reactors." *MCEER-23-0003*, University at Buffalo, Buffalo, NY.

Yu, C.-C., Whittaker, A. S., Carmichael, B. M., Chisholm, B. M., and Bolisetti, C. (2023b). "Dynamic response of base-isolated nuclear power plants for extreme ground shaking with considerations of impact." *Earthqauke Spectra*, Under review.

Yu, C.-C., Whittaker, A. S., Kosbab, B. D., and Tehrani, P. K. (2023c). "Earthquake-induced impact of base-isolated buildings: theory, numerical modeling, and design solutions." *Earthquake Engineering and Structural Dynamics*, 52, 1445-1462.